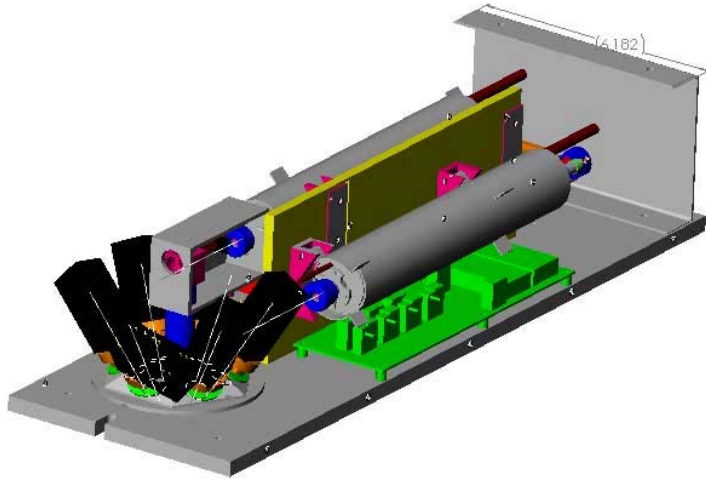


□ **Targeted Ultraviolet Chemical Sensor**

Targeted Ultraviolet Chemical Sensors (TUCS) are in-situ, non-contact, non-invasive, non-destructive sensors that require no sample handling or preparation. They employ UV laser induced native fluorescence and resonance Raman spectroscopy to detect and classify unknown molecules and molecular structures. By employing deep UV excitation wavelengths the need for tagging target materials with dyes is eliminated. Dye tags are a significant source of error in many measurements and can obscure the chemistry being measured. Using excitation wavelengths below 250nm, native or endogenous fluorescence and UV Raman emission of target molecules can be measured simultaneously without mutual interference.



Sensitivity and Specificity

Fluorescence Limit of Detection of this sensor is as low as one microorganism at a working distance of 45cm or 100 TRP molecules at a distance of 4cm. Other organic molecules such as BTEX have sensitivity in the PPT range. Resonance Raman sensitivity is about 1000 times lower. Specificity will be discussed later.

Applications:

TUCS are designed to be employed as sensitive, in situ, autonomous, industrial or environmental monitors. The sensors developed by Photon Systems operate in the deep ultraviolet to enhance their sensitivity and specificity in identifying certain molecular structures such as organic molecules and well as other molecules that are optimally excited in the UV to emit fluorescence and Raman.

Typical applications for TUCS instruments include in situ, real time measurement and characterization:

- Homeland security detectors for biological and chemical weapons materials;
- Ultrasensitive organic surface contamination detection in high quality optical fabrication, operating room surface inspection, etc.
- Cleaning validation for ultra-sensitive reagent applications
- Water quality in waste treatment plants where the content of nitrates, nitrites, carbonates, aluminates, and other water quality contaminants need to be measured on a regular basis;
- Well water or ocean water quality: sea farming, well water testing, domestic water quality;
- Chemical and microbial detection and identification in water, air and or surfaces
- Quality measurement of synthetic chemical vapor deposited diamond and diamond like carbon films in hard disc drive, super abrasives manufacturing, and other synthetic diamond applications;
- Quality measurement of epitaxial films employed in microelectronics manufacturing; substrate surface quality.
- Quality measurement of the surface condition, chemistry and quality of other elements of microelectronic devices;
- General measurement of targeted chemical compositions in quality control measurements in manufacturing such as adhesives, plastics, organic chemicals, etc

PHOTON
S Y S T E M S

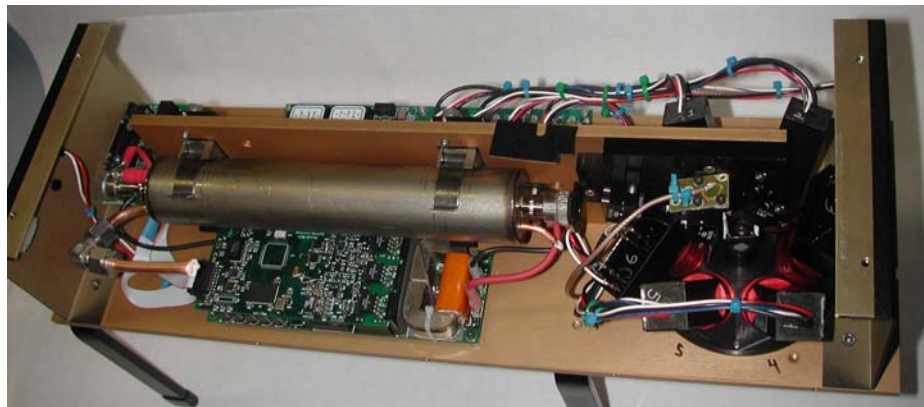
www.photonsystems.com

1512 Industrial Park St., Covina, CA 91722 T: 626 967-6431 F: 626 967-5813

Specification:

Self-contained deep UV Chemical Sensor containing:

- High power deep UV laser with power supply and digital controller capable of data sampling rates to 30 Hz.
- Spectral isolation filter for excitation wavelength
- Laser excitation power reference detector
- 6 high gain miniature PMT detection channels used to simultaneously detect a combination of laser induced native fluorescence and Raman emissions.
- A choice of number of fluorescence detection channels with selectable band center, bandwidth and slope matched to the chemical environment of the sensor.
- 7 channel PMT controller with digital gated boxcar integrator and averager containing 64MIP microprocessor with 256K RAM and 256K flash memory.
- Power: 5W standby, 6W full power – can be operated by battery or solar cell array.
- Voltage: 24VDC from battery or line source
- Size: 6” x 4” x 14”
- Weight: 5 lbs
- Control: Ethernet, IEEE485, or RF
- Software: Labview VI operated from PDA or other computer



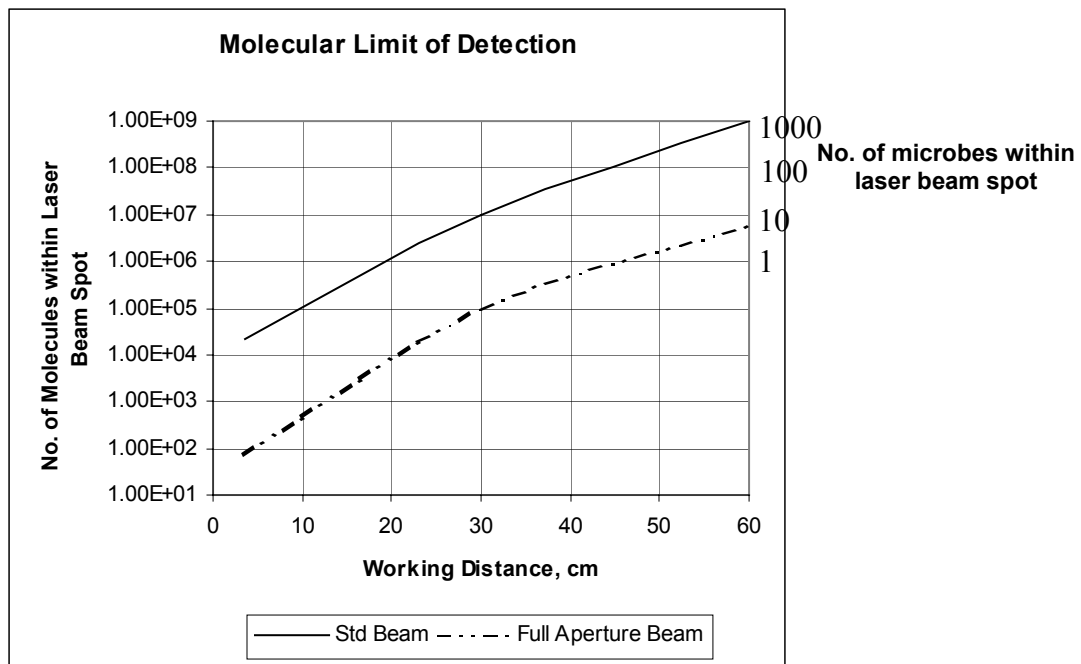
Photos of Targeted UV Chemical Sensor

PHOTON
S Y S T E M S

www.photonsystems.com
1512 Industrial Park St., Covina, CA 91722 T: 626 967-6431 F: 626 967-5813



Photo of 6 Channel Detection Aperture



Fluorescence Limit of Detection (FLOD) for tryptophane molecules and whole microorganisms versus Working Distance

Background on UV laser induced resonance Raman and resonance fluorescence

High levels of chemical specificity can be obtained using Raman spectroscopy without sample preparation, contact, or destruction¹. Raman scattering is, in general, a very inefficient process. Normal Raman scatter cross-sections are about 10^{-26} cm² for a major Raman line (1615 cm⁻¹) of a typical microorganism². Normal Raman occurs when the excitation wavelength is far from an electronic absorption band of the material. If the excitation wavelength is within a major electronic absorption band associated with the 1615 cm⁻¹ Raman band, the scattering signal is “resonance” enhanced by as much as eight (8) orders or magnitude, such that the scatter cross-section improves to about 10^{-18} cm². In contrast, maximum resonance (native) fluorescence cross-sections for the same microorganism, measured over a 30nm wide bandwidth near the peak of fluorescence, are about 10^{-11} cm². This is a factor of 10^7 improvement over resonance Raman and clearly demonstrates the sensitivity of resonance fluorescence compared to resonance Raman. However, much higher levels of specificity can be obtained with Raman.

Resonance bands for nucleic and aromatic amino acids occur in the deep UV between about 220nm and 280nm. When excited at wavelengths less than 250nm, Raman scattering occurs within about 20nm to 30nm above the excitation wavelength, corresponding to about 4000 cm⁻¹. Fluorescence occurs only above about 280nm, independent of excitation wavelength. Between the excitation wavelength at about 280nm, there exists a fluorescence-free region in which to observe the weak Raman scattering signal. A Raman shift of 4000 cm⁻¹ corresponds to a wavelength of 247nm when excited at 225nm, 278nm when excited at 250nm and 298nm when excited at 266nm. It is therefore ideal to combine UV resonance fluorescence and resonance Raman spectroscopy to form an integrated tool for both detection and identification of biological agents since they offer a great combination of sensitivity and specificity that do not share overlapping observation wavebands.

Although resonance fluorescence is not the specific subject of this program, it is an integral part of the overall detection method and is closely tied to the excitation wavelengths used for resonance Raman excitation. Therefore we will include a brief discussion of resonance fluorescence here also.

UV Resonance Fluorescence Detection of Biological Agents

All microorganisms require continual input of free energy through cellular metabolism. The source of this energy input is electrochemical potential between electron donors and acceptors. The primary carrier of free energy is adenosine triphosphate (ATP), which is derived from the oxidation of fuel molecules such as carbohydrates and fatty acids. Typical molecules responsible for the transport of energy within cells are porphyrins, quinones, flavins, NADH, etc. Other essential building blocks of living organisms are nucleic acids, amino acids and peptides, sugars and lipids, and polysaccharides. Most of

¹ Cary, P.R. (1982) *Biological applications of Raman and resonance Raman spectroscopies*, Academic Press, New York.

² Wilfred Nelson, U.Rhode Island, private communications.



these organic molecules contain chromophores which, when excited at an appropriate wavelength, will provide a signature of the material and give a good indication of the general class to which the microorganism or organic material belongs. Many other organic and inorganic materials also fluoresce that are not harmful to humans. However, when the excitation and emission wavebands are carefully chosen, these can be discriminated against with high reliability.

Optimum Fluorescence Excitation and Observation Wavelengths

Resonance fluorescence of biological agents is likely the only technique sufficiently sensitive to discover, *in situ* without any sample preparation, the presence and rough classification of a single or few numbers of microorganisms. It is the only viable method of performing non-contact biological classification of aerosols *in situ*³ because of the small dwell time for observation in an aerosol stream.

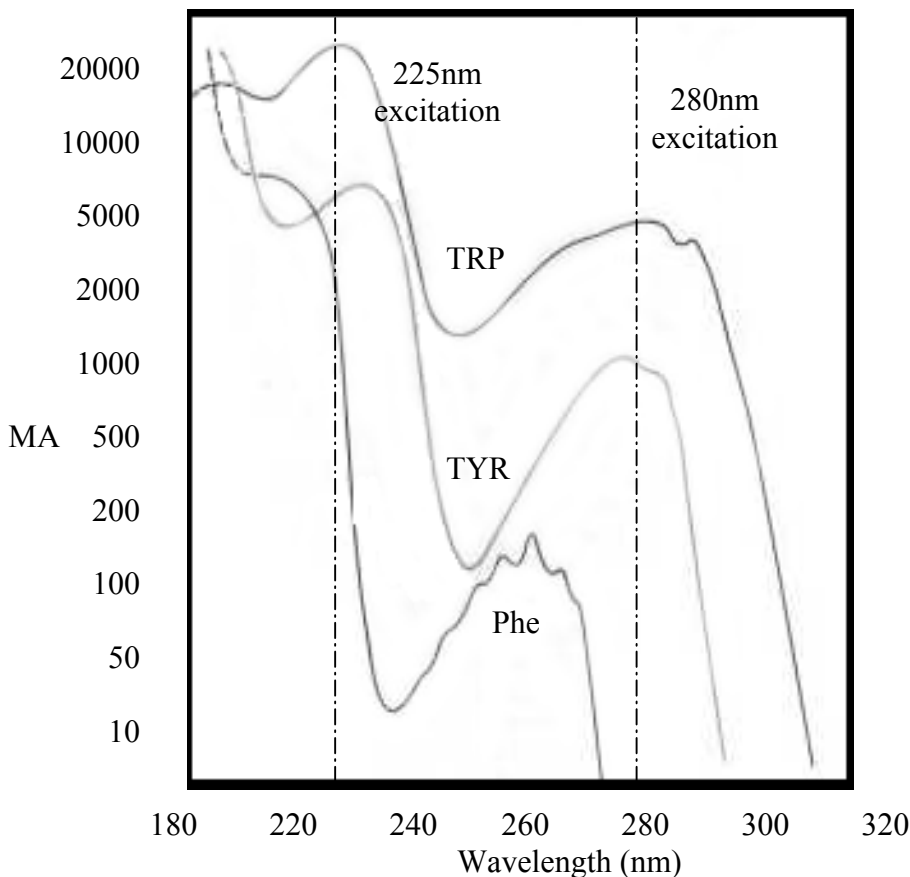


Figure 1. Molar Absorptivity of aromatic amino acids

Fluorescence emission always occurs at wavelengths longer than the excitation wavelength. Fluorescence cross-sections are a function of both the emission and excitation wavelength. If excitation occurs outside of an absorption band, the cross-section will be low, no matter how low the excitation wavelength. It is possible to select an excitation wavelength to emphasize the contrast or targeted biological agents against a wide array of potential background materials. The fluorescence spectrum of a molecule is generally a mirror image of its absorption spectrum and usually forms in broad bands, dependent on the vibrational, rotational and electronic energy level

³ Faris, G.W., R.A. Copeland, K. Mortelmans, and B.V.Bronk, "Spectrally resolved absolute fluorescence cross sections for bacillus spores", App.Opt.,Vol.36, No.4, pp.958-967, 1 February 1997.

structure of the atom or molecule and its surroundings.

Figure 1 shows the molar absorptivity of the major aromatic amino acids⁴. Note that the molar absorptivity peaks for Trp about 225nm and for Tyr about 230nm. Trp absorption at 225nm is 5 to 10 times stronger than in the traditional excitation wavelength at 280nm. The fluorescence cross-section and related efficiency is similarly higher when excited near their optima. It is a common notion that excitation at shorter wavelengths causes more interference with background materials. This is incorrect as will be shown below. The fluorescence cross-section and subsequent emission intensity is a function of both excitation and emission wavelength. This is illustrated in the following Excitation-Emission-Matrix (EEM) diagrams. EEM diagrams display the fluorescence intensity or cross-section as a function of both excitation and emission wavelength with the iso-intensity shown as contour lines, as illustrated below in Fig. 2 for *Bacillus subtilis* in both the vegetative and spore form.

It is important to note that both the spores the vegetative cells have two optimum excitation wavelengths, one near 230nm and one near 280nm. Emission maxima vegetative cells at both excitation wavelengths are the same, at about 330nm, as expected. The EEM diagram for *Bacillus subtilis* in spore form (@ 10^4 per ml) is also shown in Fig. 2. Optimum excitation wavelengths are essentially the same for *B. subtilis* spores and vegetative cell. However, the optimum emission wavelength for spores is close to 305nm compared to 340nm for vegetative cells. This is a clearly distinguishable marker feature of spores.

⁴ Thomas E. Creighton, **Proteins, Structures and Molecular Properties**, (W.H. Freeman and Company, New York, 1993)

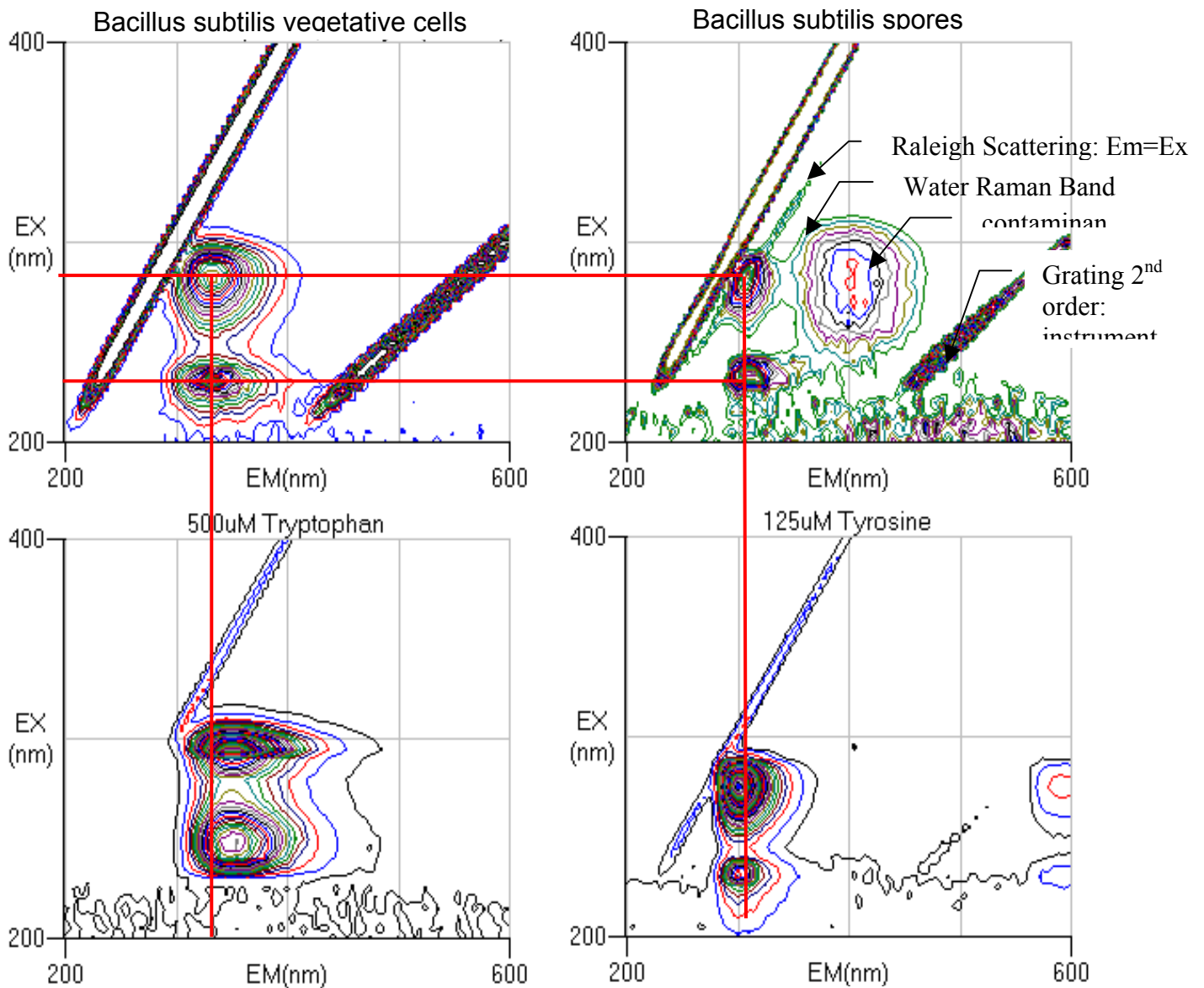


Figure 2. EEM diagrams of *B.subtilis* in spore and vegetative form with Trp and Tyr EEM diagrams

Driks⁵ shows that the spore coat for *B. subtilis* is dominated by tyrosine, whose fluorescence signature peaks near 300nm rather than the tryptophan, whose peak is near 350nm. This is shown by comparison with the TRP and TYR EEM diagrams shown below the *B. subtilis* in Fig. 2 above. A secondary optima occurring at Ex=280nm and EM=400nm is a result of a denatured alcohol contaminant in the sample. Below in Fig. 3 are the EEM diagrams of several common background materials and minerals. From the above EEM diagrams it is evident that *B.subtilis* vegetative cell fluorescence occurs at

⁵ Driks, A., "Bacillus subtilis spore coat", Microbiology and Molecular Biology Reviews, Vol.63, No.1, pp.1-20, Mar. 1999.

shorter wavelengths than pure Trp and long wavelengths than pure Tyr. The spore form is very closely related to Tyr as described by Driks.

The EEM diagrams in Fig. 3, below, illustrate the broad variation of fluorescence fingerprints of many common materials. Most materials exhibit one to three fluorescence peaks. Paper has strong peaks in the blue/green due to doping of paper with fluorescent dyes to enhance “whiteness”. The EEM fingerprints of any of these materials are significantly different from *B. subtilis* in either the spore or vegetative form. However, when detection is accomplished using a single excitation wavelength, some similarities do exist. When excited near 280nm, the emission spectrum of several plastics is similar to *B. subtilis*. However, when excited near 230nm, the spectrum is distinctly different. What is of interest is to select an excitation wavelength and a set of emission observation wavelengths for which biological agents have the highest possible differential

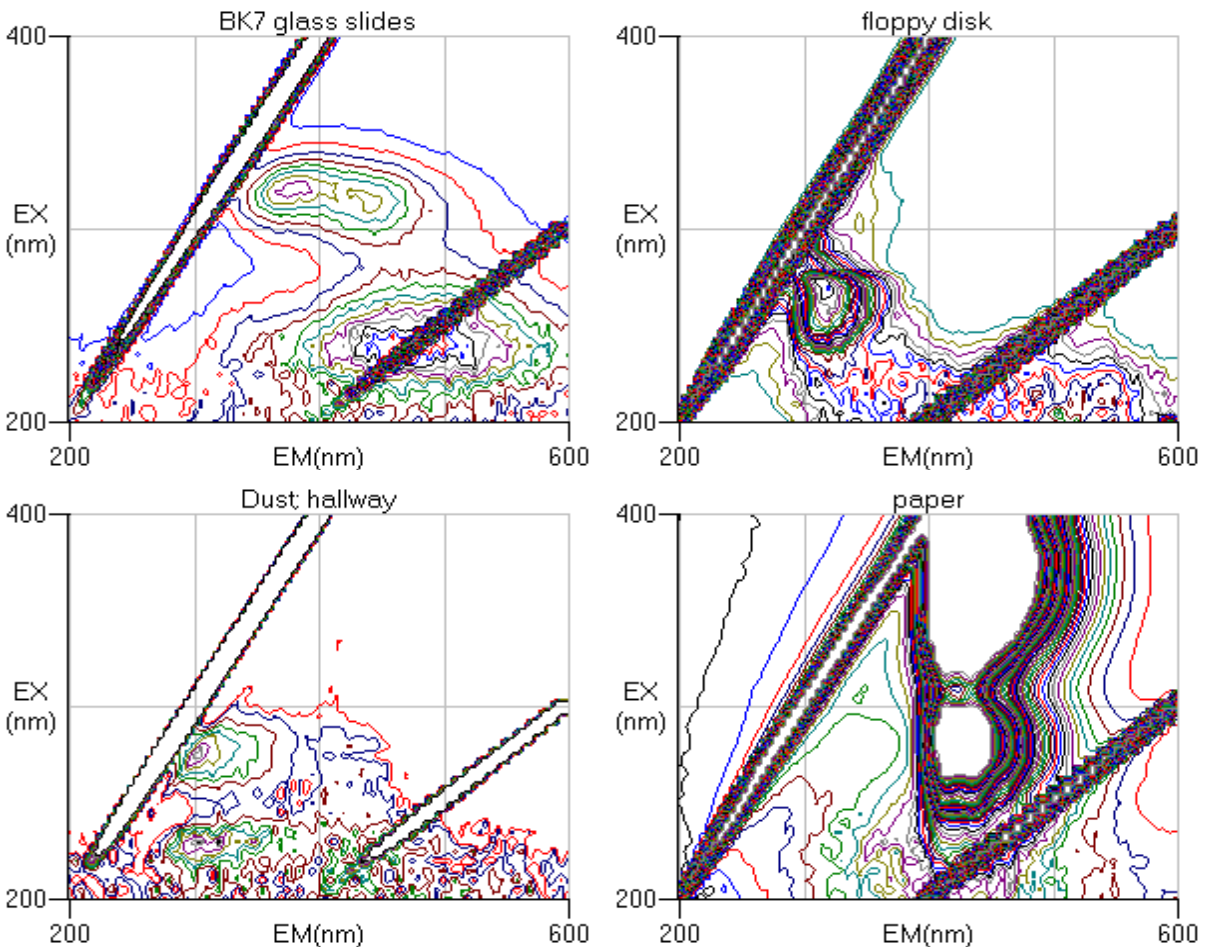


Figure 3. EEM diagrams for sample background materials

fluorescence against the widest range of background materials. It is clear from the above data that deeper UV excitation wavelengths do not “excite everything” as is commonly suggested.

Although fluorescence is not known for its chemical specificity, by choice of the number of spectral detection bands and their bandwidth and band location, a significant level of chemical specificity can be achieved. Below, in Fig. 4, six detection bands are shown that are used in our TUCS instrument. We can alter these bands but the following selection is a good example of what level of specificity is achievable.

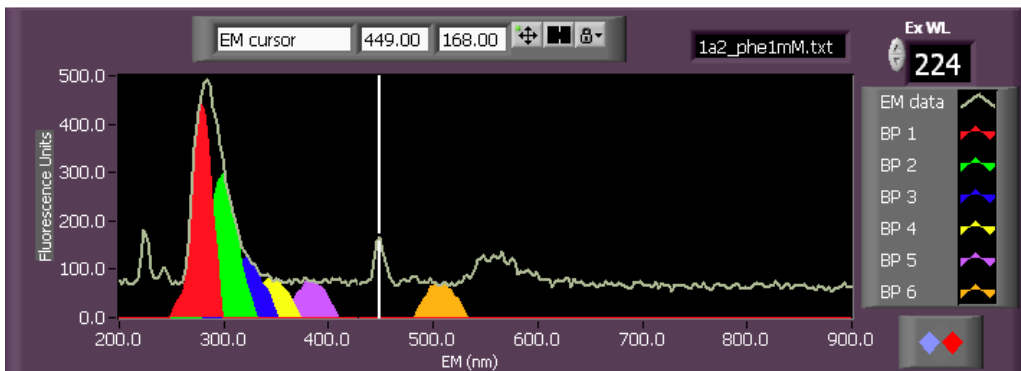


Figure 4. Illustration of six resonance fluorescence detection bands

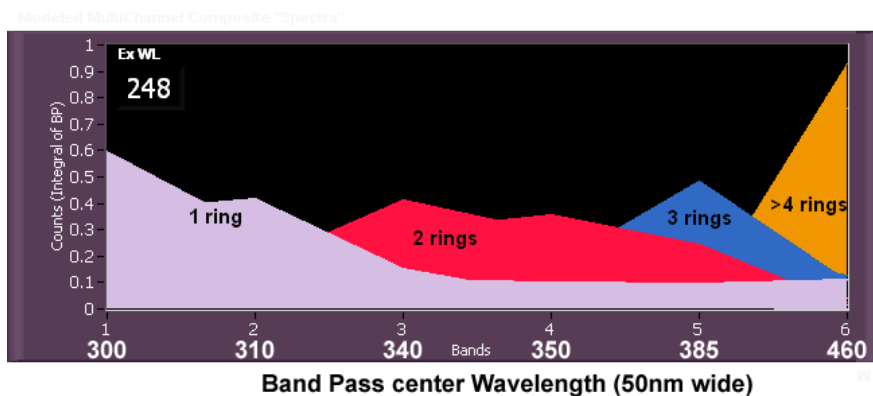
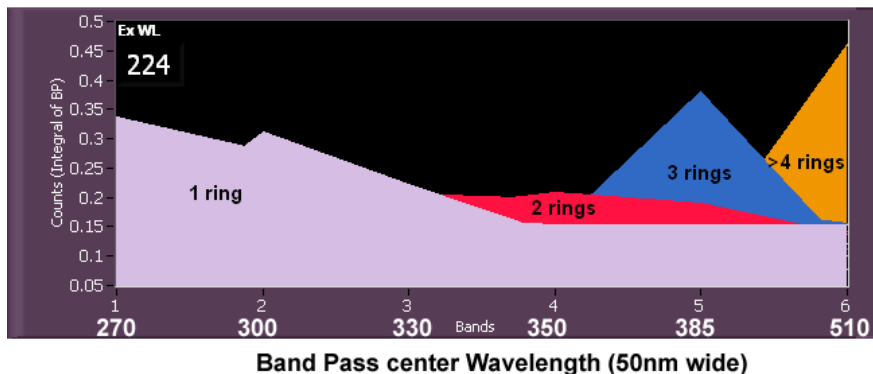


Figure 5. Resonance fluorescence for 1 through 4 ring chemical structures with excitation at 224nm and 248nm. (Courtesy of Pan Conrad and Rohit Bhartia, Caltech/JPL)

The following figure shows the ability to distinguish multi-ring polycyclic aromatic hydrocarbons using resonance fluorescence measured in six bands.

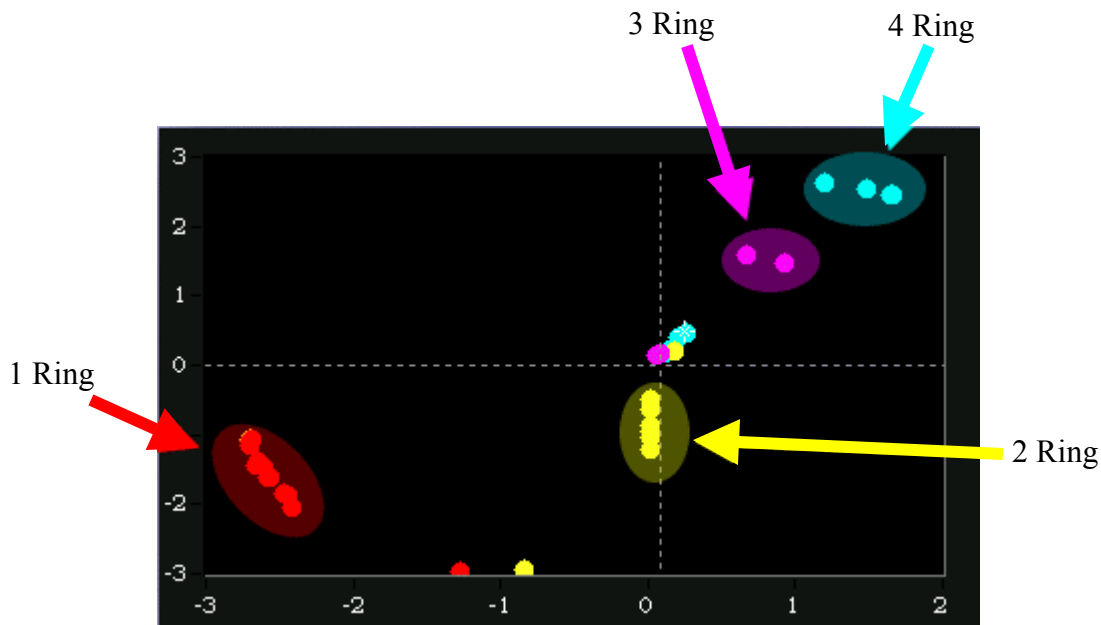


Figure 6. Six-band resonance fluorescence detection and classification of polycyclic aromatic hydrocarbons using simple band differencing algorithm. (Courtesy of Pan Conrad and Rohit Bhartia, Caltech/JPL)

Forty three (43) different PAH's are compared in the above illustration. Variances within each Ring Group are due to functional groups (-methyl, dimethyl, etc.). Outliers are a result of addition of conjugated bonds (C=C) or non-aromatic rings.

Although we are far from optimizing the performance of this instrument, Fig. 6 demonstrates a considerable level of specificity, while at the same time having sensitivity better than one femtomole ($1/10^{15}$) and perhaps as high as one attomole ($1/10^{18}$).

Within each Ring Group we are able to further differentiate molecules such as aromatic amino acids from single benzene-ring structures. We are able to clearly differentiate between spores, vegetative cells and virus'. And these can be clearly differentiated from minerals and other background materials.

UV Resonance Raman Identification of Biological Agents

Over the past ten years UV resonance Raman spectroscopy has been increasingly used for detection and identification of microorganisms and study of cellular function⁶⁷⁸⁹¹⁰. UV resonance Raman spectroscopy allow the measurement of clear band structures within the electronic absorption manifold of the target biological molecules and thereby enables the ability to more clearly characterize unknown biological materials. Photon Systems has benefited from close collaborations and association with Professors Sanford Asher of the University of Pittsburgh and Wilfred Nelson of the University of Rhode Island in conjunction with our development of deep UV lasers and miniature Raman instruments. Both of these men are known for their groundbreaking work in UV resonance Raman spectroscopy, especially as it applies to characterization of organic molecules and the molecules of life. We recently published a paper with Prof. Asher¹¹.

It has been clear for several years that unique ultraviolet resonance Raman spectral signatures can reliably be detected in as few as 20 bacterial cells with low power consumption and low photon flux levels (Nelson, 1993¹²; Nelson, et.al¹³, 1993; Chadha, et.al., 1993¹⁴). In fact, UVRR has made possible the detection and characterization of single cells.

Taxonomic Raman Marker Bands

A summary of the major taxonomic marker bands of highly degenerate functional groups occurring within microorganisms is shown below in Table I.

Table I. Major Taxonomic Raman marker bands for biological agents

Material	Raman Band Locations					
Tryptophan	753	879	1011	1353	1555	1615
Tyrosine	831	852	1180	1210		1615
Guanine				1320 1365	1485	1577 1603
Adenine				1337	1485	1580
Cytosine					1530	
Dipicolinic Acid			1017	1195	1396	1446

⁶W.H.Nelson, R. Manoharan and J.F. Sperry, "UV Resonance Raman Studies of Bacteria", *App. Spect. Reviews*, 27 (1), pp67-124, 1992

⁷S. Chadha, W. H. Nelson and J.F. Sperry, "Ultraviolet micro-Raman spectrograph for the detection of small numbers of bacterial cells", *Rev. Sci. Instrum.* 64 (11), pp.3088-3093, Nov. 1993

⁸Z. Chi and S. A. Asher, "UV resonance Raman Determination of Protein Acid Denaturation", *Biochemistry*, 37, pp.2865-2872, 1998.

⁹N.Cho and S.A. Asher, "UV resonance Raman studies of DNA-Pyrene interactions", *J.Am. Chem.Soc.* 115, pp.6349-6356, 1993

¹⁰F. Sureau, et.al., "An ultraviolet micro-Raman spectrometer: Resonance Raman spectroscopy within a single cell", *App.Spect.*, 44, No.6, pp.1047-1051, 1990

¹¹Sparrow, M.C., J.F. Jackovitz, C.H. Munro, W.F. Hug, and S.A. Asher, "A New 224nm Hollow Cathode UV Laser Raman Spectrometer", *J. App. Spectroscopy*, Vol. 55, No. 1, Jan 2001.

¹²Nelson, W.H. (1993) *Rev. Sci. Inst.* (11):3088-3093

¹³Nelson, W.H., Manoharan, R., and Sperry, J.F. (1992) *Appl. Spect. Rev.* 27(1), 67

¹⁴Chadha, S., Nelson, W.H., Sperry, J.F. (1993) *Rev. Sci. Inst.* (11):3088-3093

Identification of biopolymers or organisms using UV Raman spectroscopy depends on the ability to produce interpretable, reproducible spectra. DNA and cell surface antigens are the most attractive targets as potential markers for cellular or bacterial identification. Identification of organisms using UV Raman spectroscopy has focused on the ratio of a few taxonomic marker bands (Ref.13). These band markers are based on ratios of tryptophan and tyrosine and DNA base pairs that can be characteristic of an organism. As mentioned previously, most biological materials have repeating functional groups that are highly degenerate. These include nucleic acid base pairs and aromatic amino acids. These repeating units have Raman spectra that are very similar to the spectra of the monomers upon which they are based. Raman spectra of *B. cereus* in several forms is shown below in Fig. 7 in using 242nm excitation: vegetative, spore and germinated spore (Ref.13). Major Raman marker bands are shown at 1019 cm^{-1} , 1485 cm^{-1} , 1530 cm^{-1} , 1555 cm^{-1} , and 1615 cm^{-1} . The measurement bandwidth illustrated is about 25 cm^{-1} .

Bacteria can be characterized as Gram positive versus Gram negative based on the 1555 cm^{-1} /1615 cm^{-1} intensity ratio. Gram negative bacteria have a much higher ratio of the tryptophan intensity at 1011 cm^{-1} or 1555 cm^{-1} compared to the Tyr + Trp intensity at 1615 cm^{-1} . In general, this ratio is described as the intensity in broad spectral regions centered near the 1555 cm^{-1} and 1615 cm^{-1} Raman bands. However, the exact position, center of gravity, band width, and other features of each band can provide more detailed identification of bacteria. However, the relationships are presently unknown. It is believed that these marker bands primarily describe the

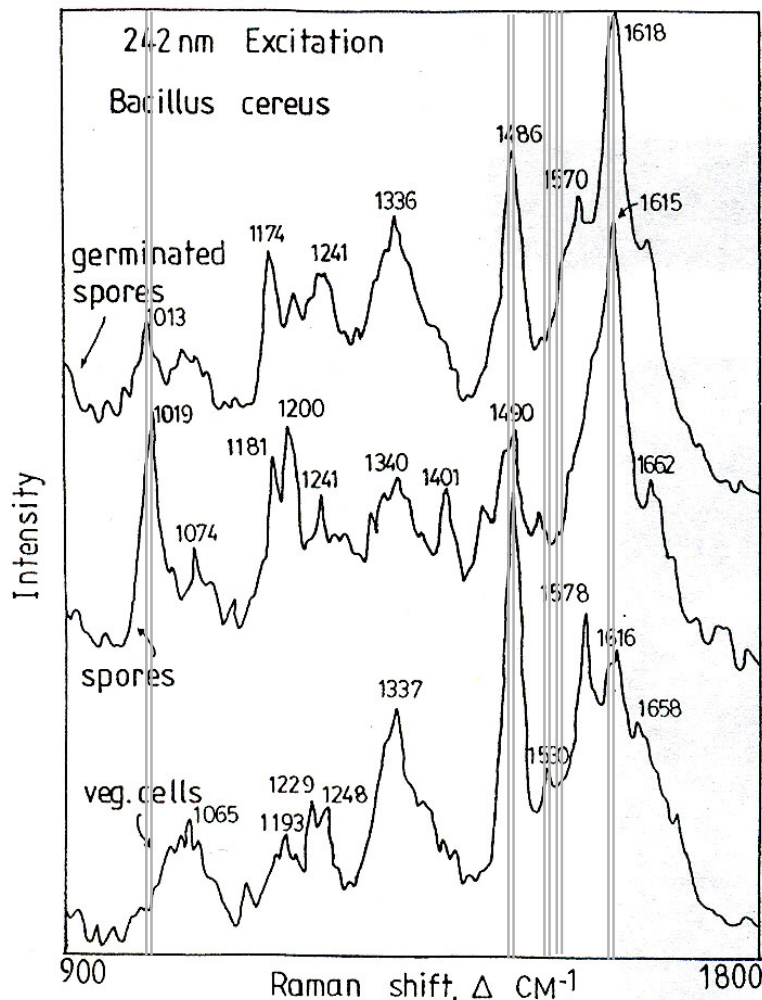


Figure 7. Resonance Raman spectra of *B. cereus* in various

surface composition of an organism.

Within Gram positive organisms such as spores, or vegetative cells there is further sub-classification G+C percentage. This is determined by the $1530\text{ cm}^{-1}/1485\text{ cm}^{-1}$ Raman band intensity ratio. The intensity of the 1485 cm^{-1} peak is taken as closely proportional to the total amount of nucleic acid on a molar basis (DNA + RNA) in the cell. The intensity of the peak at 1530 cm^{-1} can be assumed to be proportional to the moles of cytosine in the nucleic acids. It follows that the mole fraction of G+C in the bacteria should be proportional to the ratio of the 1530 cm^{-1} and 1485 cm^{-1} peaks.

Following is a graph of the $1530/1485\text{ cm}^{-1}$ ratio versus the known percentage of G+C of DNA in 14 different bacterial species grown on TSA and in TSB, respectively (Ref.13). The peak intensity ratios versus molar percent G+C are linear dependent, as shown in Fig. 8.

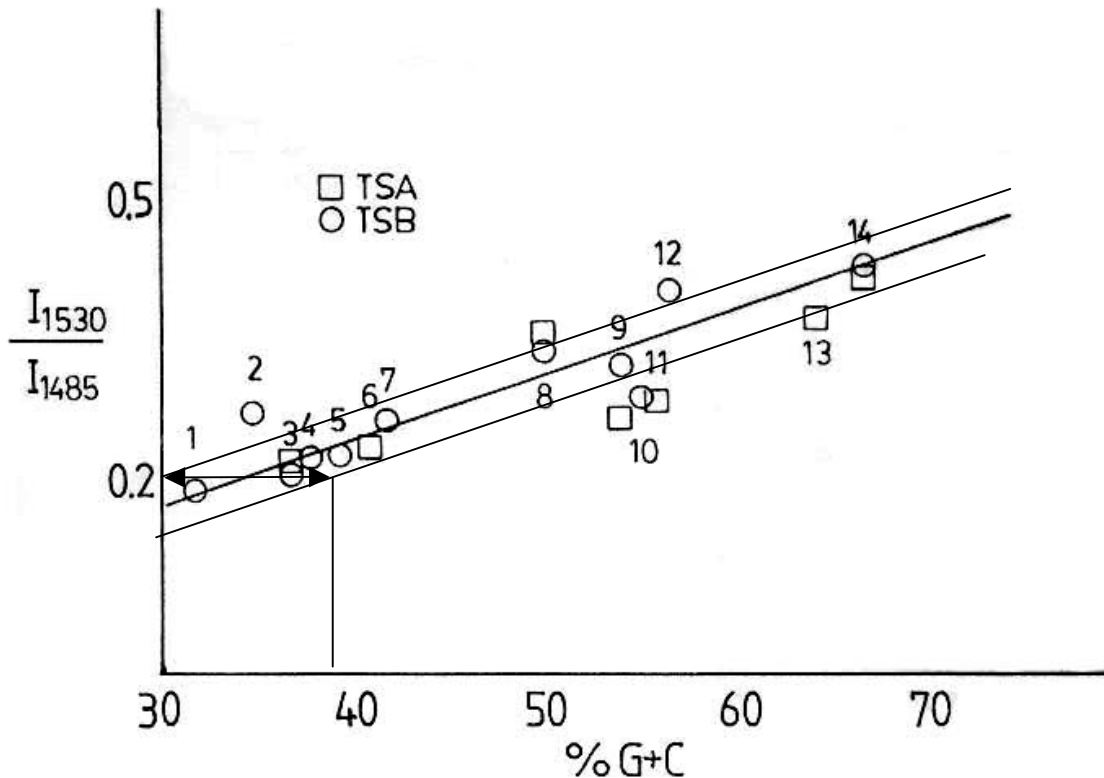


Figure 8. Plot of $1530\text{ cm}^{-1}/1485\text{ cm}^{-1}$ versus known G+C for 14 bacterial species. 242nm excitation. (Adapted from Ref.13)

Three lines are shown in Fig. 8 which represent the mean and \pm one standard deviation of the data. This preliminary estimate illustrates the potential to identify an organism within about ± 3 to ± 5 mole percent G+C. In combination with identification of the Gram polarity and whether the organism is a spore, the G+C content can provide significant specificity in identification or biological agents. The organisms employed in Fig. 8 are tabulated below in Table II.

Table II. DNA mole fraction for Guanine + Cytosine for bacteria in Fig. 8

Plot No.	Organism	Mole% G+C	Gram	Spores	Virulence class ^g
	<i>Clostridium botulinum</i>	28.2 ⁱ	+	X	2
	<i>Rickettsia prowasecki</i>	28.9 ⁱ	-		3
	<i>Staphylococcus aureus</i>	32.8 ^b	+		2
1	<i>Bacillus cereus</i>	32 ^a	+	X	1
2	<i>Enterococcus faecalis</i>	34-36 ^a 37.5 ^b	-		1
	<i>Staphylococcus simulans</i>	34-38 ^a	+		1
	<i>Bacillus anthracis</i> Ames	35.2 ^b	+	X	2
	<i>Streptococcus agalactiae</i>	35.5 ^b	+		1
4	<i>Proteus vulgaris</i>	36-40 ^a	-		1
3	<i>Bacillus magaterium</i>	37 ^a	+	X	1
5	<i>Proteus mirabilis</i>	39.5 ^a	-		1
6	<i>Bacillus subtilis</i>	41 ^a	+	X	1
7	<i>Acinetobacter calcoaceticus</i>	42 ^a	-		2
	<i>Bacillus subtilis</i>	43.5 ^b	+	X	1
	<i>Shewanella oneidensis</i> MR1	45.9 ^b	-		1
	<i>Yersinia pestis</i> .	47.6 ⁱ	-		3
	<i>Vibrio cholerae</i>	47.6 ⁱ	-		3
8	<i>Escherichia coli</i> , K12-MG1655	50.7 ^b	-		2
	<i>Shigella dysenteriae</i>	50 ⁱ	-		2
	<i>Samonella tphi</i>	52.1 ⁱ	-		2
9	<i>Enterobacter aerogenes</i>	54.3 ^a	-		1
10	<i>Alcaligenes faecalis</i>	54.8 ^a	-		1
11	<i>Enterobacter cloacae</i>	55.4 ^a 57.2 ^b	-		1
12	<i>Aeromonas hydrophila</i>	55.7 ^a	-		1
	<i>Brucella suis</i> 1330	57.2 ^b	-		3
	<i>Brucella melitensis</i>	57.2 ^c	-		3
	<i>Aeromonas hydrophila</i>	59-62 ^c	-		1
	<i>Pseudomonas putida</i>	61.4	-		1
13	<i>Pseudomonas aeruginosa</i>	64 ^a , 66.4 ^b	-		1
14	<i>Micrococcus luteus</i>	66.3 ^a	+		1
	<i>Alcaligenes faecalis</i>	66.7-69.9 ^c	-		1
	<i>Burkholderia pseudomallei</i>	68.06 ⁱ	-		3

a=A.I.Laskin & H.A.Lechevallier(eds), CRC Handbook of Microbiology, Vol.II, CRS Press, Cleveland, 1973. b=tigr, i=Sanger Inst.

Biological Agent Identification Specificity

One possible detection and identification strategy for biological agents using laser induced resonance fluorescence and UV Raman spectroscopy is as follows:

- a. Determine if a particle is biological or non-biological based on laser induced resonance fluorescence measured in the 300nm region.
- b. If particle is biological, measure the relative UV Raman intensity at five (5) Raman bands centered at 1017 cm^{-1} , 1485 cm^{-1} , 1530 cm^{-1} , 1555 cm^{-1} and 1615 cm^{-1} .
- c. Determine if the particle is Gram positive or negative based $1555\text{ cm}^{-1}/1615\text{ cm}^{-1}$ ratio.
- d. Determine if the particle is a spore based on the $1017\text{ cm}^{-1}/1615\text{ cm}^{-1}$ ratio.
- e. Determine the GC% based on the $1530\text{ cm}^{-1}/1485\text{ cm}^{-1}$ ratio.

Measurement of the Raman scattering in only five (5) broad ($\approx 40\text{cm}^{-1}$) bands ***provides knowledge of the: Gram polarity; form of organism; and G+C percent.*** These measurements can be made rapidly and correlated using any of several artificial neural net or PCA/PCO algorithms to give a relatively high degree of confidence in identifying organisms within a narrow range. These measurements could be made in sub-second time scales and possibly as short as a millisecond or faster.

Using this fast and simple 5-band Raman technique, it would appear that it is unlikely this method would be able to specifically differentiate *B. anthracis* against a background containing a wide range of other similar spore interferants since the detection accuracy corresponds to only about $\pm 4\%$ in G+C concentration. The closest spore to *B. anthracis* at GC=35.2% is *B. cereus* at 32% ($\Delta=3.2\%$) and *B. magisterium* at 37% ($\Delta=1.8\%$). All three are spore formers and all are Gram positive. So none of the discriminators would have differentiated between these organisms with a low false alarm rate. However, this fast method will probably enable discrimination of *B. subtilis* from *B. anthracis*. In addition, this method would be able to discriminate anthrax from a wide range of other bacterial spores and other microorganisms and identify them within a small range.

There are many UV Raman spectroscopic options that have yet to be evaluated to reduce the false alarm rate in identifying *B. anthracis* or other virulent microorganisms. The fast and simple approach described above does not take advantage of the much larger wealth of information contained in UV Raman spectra. Substantial differences in taxonomic marker band intensity, peak position, center of gravity, and band shape occur for each of the basic Raman marker bands. These are a result of environmental and conformational differences between organisms as well as more subtle compositional differences. In addition, there are other Raman marker bands that are clearly measurable which may give further discrimination to microorganism identification. In order to provide a higher level of biological agent specificity, higher resolution Raman spectra would be required. A reasonable way to triage a target would be to follow the laser induced resonance fluorescence and broadband UV resonance Raman with high resolution UV resonance Raman. Each of these techniques is successively more time consuming, less sensitive



www.photonsystems.com

1512 Industrial Park St., Covina, CA 91722 T: 626 967-6431 F: 626 967-5813

and more specific. At present there is no clear model to provide higher specificity based on more subtle nuances of the Raman spectra such as peak position or center of gravity variations due to difference in microorganisms....but we're working on it.



www.photonsystems.com
1512 Industrial Park St., Covina, CA 91722 T: 626 967-6431 F: 626 967-5813